

Correlation of Damage of Steel Moment-Resisting Frames to a Vector-valued Ground Motion Parameter Set that includes Energy Demands: Collaborative Research of the University of Texas at Austin (UT) and Applied Insurance Research (AIR).

AWARD No. 03HQGR0106

Dr. Lance Manuel and Mr. Sridhar Baldava

Dept. of Civil Engineering
University of Texas at Austin
Austin, TX 78712
512/232-5691 (phone)
512/471-7259 (fax)
lmanuel@mail.utexas.edu
sridharb@mail.utexas.edu

in collaboration with

Dr. Paolo Bazzurro and Dr. Nicolas Luco (AIR)

Keywords: Structural building response; strong ground motion; probabilistic seismic hazard; loss estimation.

INVESTIGATIONS UNDERTAKEN

This study investigates the correlation of structural response measures with different combinations of ground motion parameters that include energy-based quantities. The final purpose is to improve the prediction of structural behavior during earthquakes. A more accurate assessment of seismic performance of buildings is of paramount importance for designing new safer structures and for evaluating whether existing ones should be retrofitted to guarantee an acceptable level of safety to occupants. In addition, better performance assessment capabilities will enable one to improve the prediction of earthquake-generated losses. The availability of reliable loss estimates is crucial to different stakeholders such as owners, tenants, insurance and reinsurance companies, and public organizations for post-earthquake emergency resource management.

This study is empirical in nature. We consider 140 real ground motion recordings from earthquakes of engineering interest – namely intermediate- to large-magnitudes events (with moment magnitude, M , between 5.7 and 7.5) recorded at moderate distances (taken here to be less than 36km from the causative fault). This ground motion dataset is applied to low-rise (3-story), a mid-rise (9-story), and a high-rise (20-story) steel moment-resisting frame (SMRF) buildings designed for Los Angeles conditions as part of Phase II of the SAC Project (FEMA-355C, 2000). To distinguish between the performance of older-vintage SMRF buildings before and after retrofitting, we consider both a brittle model (that allows for beam-column connection fracture, a phenomenon widely observed in the 1994 Northridge earthquake) and a ductile model (that mimics the behavior of a retrofitted SMRF building). The response of these buildings to the 140 records is computed via nonlinear dynamic analysis using the computer program, Ruaumoko (Carr, 2003).

The novelty of this study is two-fold:

1. We intend to investigate the predictive power of different combinations of ground motion parameters that include **both** conventional elastic spectral parameters (e.g., spectral acceleration, S_a , at the initial fundamental frequency of the structure and at higher modes) as well as energy-based parameters (e.g., input energy). (Uang and Bertero, 1990.)
2. We intend to predict not one single response measure (e.g., the roof drift or the maximum inter-story drift over the height of the building) but a vector of measures (e.g., the peak inter-story drifts at all stories) whose components will, in general, be correlated. The knowledge of more than one measure, simultaneously, of building performance is expected to improve the accuracy of performance and loss assessments.

RESULTS

Task 1: Select near-source and "ordinary" earthquake ground motion records relevant to the Southern California region.

We selected the 140 ground motion records described in Tables 1 and 2 from the Pacific Earthquake Engineering Research (PEER) database. The distribution by magnitude, M , and distance, R , of the selected ground motions is summarized in the scatter plot shown in Figure 1. The selection of records was guided by the following criteria:

- With few exceptions, preference was given to records obtained from the Southern California region. Records from the 1999 Chi-Chi earthquake were excluded.
- Since smaller events are not expected to cause significant structural damage to engineered structures, priority in selection of ground motions was given to records from events with moment magnitude as large as possible. As a result, the database has no records from magnitudes smaller than 5.7.

- Records with source-to-site distance less than 16 km were selected for the "near-source" records, and in the 16-36 km range for the "ordinary" records. The division point between the two sets was made in order to have an equal number of near-source and ordinary records. Sites at distances rather away than those considered here are believed to be less at risk.
- A need to include "similar" soil conditions was felt to be important so that our conclusions are not colored by possible site response and or soil amplification effects that might result if different soil conditions were considered. Accordingly, the criterion used was that neither rock sites nor soft soil sites were to be included. Thus, effectively, only conditions similar to NEHRP C or D site classes were considered.
- Only records whose high-pass filter corner frequency used during processing was not higher than 0.2Hz were used, since the largest elastic vibration period of interest is roughly 4 seconds = $1/(1.25 \times 0.2\text{Hz})$ for the 20-story building.
(Note: The factor of 1.25 is explained at <http://peer.berkeley.edu/smcat/process.html>).
- A sufficient number of records for the planned multivariate multiple regressions to follow was estimated to be about 150. This established the size of the database employed.

We computed 5%-damped elastic response spectra and input energy spectra for the entire suite of records. Summarized in Figure 2 are response spectra (for pseudo-spectral acceleration, S_a) for all 140 records used. In Figure 3, similarly, input energy-equivalent acceleration (A_i) spectra are shown for the 140 records. Mean spectral shapes are also shown in Figures 2 and 3. As might be expected, $S_a(f)$ and $A_i(f)$, at the same oscillator frequency, f , are highly correlated (positively) with each other. This strong correlation may cause colinearity problems during regression (Johnson and Wichern, 2002). To partially remove this source of correlation, we computed the ratio, $R_{SE}(f)$, of $S_a(f)$ to $A_i(f)$. This ratio, as shown in Figure 4, appears to be far less correlated to $S_a(f)$. Therefore in subsequent investigations, we anticipate coupling, in the same regression model, either one of the strength- or energy-based parameters (i.e., S_a or A_i) with this ratio, R_{SE} .

Note that just as the 140 records have been divided into "near-source" and "ordinary" bins in order to highlight differences in the correlation of structural response to ground motion parameters for these two types of records, these 140 records may also be binned by magnitude and/or rupture-directivity (i.e., forward or backward). Such alternative bins will be considered in subsequent reporting of our results.

Task 2: Perform nonlinear dynamic analysis of the three SAC model buildings.

We have developed two variants of the nonlinear dynamic analysis computer models for the three SMRF buildings (3-story, 9-story, and 20-story) – one with brittle and the other with ductile connections.

To date, we have performed a full set of 140 nonlinear dynamic analyses for the ductile models of the 3-, 9-, and 20-story buildings. For illustration purposes, Figure 5 shows the response of the 9-story ductile model measured in terms of peak roof drift plotted versus spectral acceleration at the fundamental period, T_1 , which in this case is equal to 2.2 sec. As expected, the correlation is very strong, even into the nonlinear range (beyond a peak roof drift ratio of about 0.01). Generally speaking, higher modes (than the fundamental) do not contribute significantly to roof drift, but they can contribute to certain inter-story drifts. Figure 6 shows the variation of peak inter-story drifts over the entire height of the building for all 140 records. To visually appreciate the different degrees of response severity caused, on average, by records of different "strength," we display in Figure 7 the median deformed building shape for records binned according to first-mode spectral acceleration. Note how the drifts at the upper and lower stories grow disproportionately with the strength of the input ground motions.

The nonlinear dynamic analyses for the brittle variants of the SMRF buildings are currently in progress. A major difficulty in completing these analyses has been the less-than-satisfactory performance of the Ruaumoko software in describing brittle connection behavior. With the aid of its developer, Dr. Athol Carr, we are currently improving the Ruaumoko library element that models brittle connections in SMRF buildings.

Task 3: Perform multivariate multiple linear regression (MMLR) analysis of vector of response measures on different combinations of ground motion parameters.

This task is where the bulk of the remaining work will be concentrated until the end of the project. To date, for the ductile 9-story building, we have performed a MMLR analysis of the vector of peak inter-story drifts using three different regression models that include the spectral acceleration values at (i) the first natural frequency, $S_a(f_1)$; (ii) at the first two natural frequencies, $S_a(f_1)$ and $S_a(f_2)$; and (iii) at the first three natural frequencies, $S_a(f_1)$, $S_a(f_2)$, and $S_a(f_3)$. In lieu of $S_a(f_2)$ and $S_a(f_3)$, the ratios $S_a(f_2)/S_a(f_1)$ and $S_a(f_3)/S_a(f_2)$ have also been utilized in order to avoid the effects of colinearity on the regression that are introduced by strong correlation between more than one spectral parameter (as described above under Task 1 for $S_a(f)$ and $A_i(f)$).

Figure 8 shows the story drifts predicted by the regression model that includes $S_a(f_1)$. The values of $S_a(f_1)$ considered are the medians of the same five bins of records considered for Figure 7. Note that these regression predictions compare well with the average deformed shape empirically predicted by the records binned according to $S_a(f_1)$. Although not shown here, the MMLR analysis results for the models that include $S_a(f_2)/S_a(f_1)$ and $S_a(f_3)/S_a(f_2)$ suggest that the contribution from the second and third mode spectral values is significant when predicting peak inter-story drift ratios at some but not all of the nine stories.

NON-TECHNICAL SUMMARY

For design and performance assessments of new and existing structures in seismic areas, it is important to identify ground motion parameters that correlate to structural response and, in turn, to damage and monetary loss. Once this correlation is established, engineers can more accurately evaluate the likelihood of exceeding different specified levels of response/performance for a structure at a given site, and can then also estimate the likelihood that the structure will either collapse or suffer intermediate levels of structural damage. This study is investigating if advantages exist from using combinations of spectral and energy-based parameters to predict the structural response of low-, mid-, and high-rise steel buildings.

REPORTS PUBLISHED

None to date.

AVAILABILITY OF SEISMIC DATA

The ground motion records used in this study (Tables 1 and 2) were obtained from the Pacific Earthquake Engineering Research (PEER) database. These records are in ASCII format. The database is available online at <http://peer.berkeley.edu/smcat/index.html>. The contact name for PEER is: Parshaw Vaziri, PEER Director of PR & Outreach, Tel: 510-231-9550 or 510-301-1889.

REFERENCES

Carr, A. J., "Ruaumoko User Manual," University of Canterbury, New Zealand, 2003.

FEMA-355C, "State of the Art Report on Systems Performance of Steel Moment Frames Subject to Earthquake Ground Shaking," Federal Emergency Management Agency, September 2000.

Johnson, R. A. and D. W. Wichern, "Applied Multivariate Statistical Analysis," 5th Edition, Prentice-Hall, Inc., 2002.

Uang, C.-M. and V. V. Bertero, "Evaluation of Seismic Energy in Structures," Earthquake Engineering and Structural Dynamics, Vol. 19, pp. 77-90, 1990.

EQID	EQNAME	STANAME	YEAR	Mw	Clst Dis	X	GM Site Code	NEHRP	Filename	Max fcHP	Min fcLP	#	Strike
0048	Coyote Lake	Gilroy Array #2	1979	5.74	8.45	-1	IQD	D	COYOTELK\G02050	0.2	40	1	336
0048	Coyote Lake	Gilroy Array #3	1979	5.74	6.9	-1	IHD	D	COYOTELK\G03050	0.2	40	2	336
0048	Coyote Lake	Gilroy Array #4	1979	5.74	5.22	-1	AHD	D	COYOTELK\G04270	0.2	25	3	336
0048	Coyote Lake	Gilroy Array #6	1979	5.74	3.15	-1	IKB	C	COYOTELK\G06230	0.2	25	4	336
0102	Chalfant Valley-01	Zack Brothers Ranch	1986	5.77	6.22	1	AAD	-	CHALFANT\B-ZAK270	0.11	30	5	48
0113	Whittier Narrows-01	Garvey Res. - Control Bldg	1987	5.99	12.69	0.28	APB	-	WHITTIER\A-GRV060	0.2	40	6	280
0113	Whittier Narrows-01	Norwalk - Imp Hwy, S Grnd	1987	5.99	15.82	-0.36	IHD	-	WHITTIER\A-NOR090	0.15	40	7	280
0101	N. Palm Springs	Cabazon	1986	6.06	7.84	0.53	AHD	-	PALMSPR\CAB180	0.15	40	8	287
0101	N. Palm Springs	Morongo Valley	1986	6.06	12.07	-0.07	AHC	C	PALMSPR\MVH045	0.08	50	9	287
0025	Parkfield	Cholame - Shandon Array #12	1966	6.19	14.35	-1	IQD	C	PARKF\C12050	0.2	20	10	143
0025	Parkfield	Cholame - Shandon Array #5	1966	6.19	4.98	-0.98	IHC	D	PARKF\C05085	0.2	17.4	11	143
0025	Parkfield	Cholame - Shandon Array #8	1966	6.19	8.96	-0.99	IQD	D	PARKF\C08050	0.2	20	12	143
0025	Parkfield	Temblor pre-1969	1966	6.19	9.84	-1	IJA	C	PARKF\TMB205	0.2	14.7	13	143
0090	Morgan Hill	Anderson Dam (Downstream)	1984	6.19	3.26	-0.61	AFD	C	MORGAN\AND250	0.1	30	14	148
0090	Morgan Hill	Gilroy - Gavilan Coll.	1984	6.19	14.84	-0.98	AFB	C	MORGAN\GIL067	0.1	30	15	148
0090	Morgan Hill	Gilroy Array #2	1984	6.19	13.69	-0.98	IQD	D	MORGAN\G02000	0.2	31	16	148
0090	Morgan Hill	Gilroy Array #3	1984	6.19	13.02	-0.98	IHD	D	MORGAN\G03000	0.1	32	17	148
0090	Morgan Hill	Gilroy Array #4	1984	6.19	11.54	-0.98	AHD	D	MORGAN\G04270	0.1	25	18	148
0090	Morgan Hill	Gilroy Array #6	1984	6.19	9.87	-0.98	IKB	C	MORGAN\G06000	0.1	27	19	148
0090	Morgan Hill	Gilroy Array #7	1984	6.19	12.07	-0.98	AHB	D	MORGAN\GMR000	0.1	30	20	148
0090	Morgan Hill	Halls Valley	1984	6.19	3.48	0.02	IFC	D	MORGAN\HVRI150	0.2	26	21	148
0103	Chalfant Valley-02	Zack Brothers Ranch	1986	6.19	6.17	-0.63	AAD	-	CHALFANT\A-ZAK270	0.1	33	22	148
0064	Victoria, Mexico	Cerro Prieto	1980	6.33	6.37	0.95	AVA	C	VICT\CPE045	0.2	62.5	23	130
0064	Victoria, Mexico	Chihuahua	1980	6.33	11.5	0.95	IQD	D	VICT\CHI102	0.2	22	24	130
0076	Coalinga-01	Pleasant Valley P.P. - bldg	1983	6.36	11.83	-0.37	AHD	-	COALINGA\H-PVB045	0.2	20	25	145
0076	Coalinga-01	Pleasant Valley P.P. - yard	1983	6.36	11.83	-0.37	AHD	-	COALINGA\H-PVY045	0.2	31	26	145
0050	Imperial Valley-06	Aeropuerto Mexicali	1979	6.53	1.36	0.05	I-D	D	IMPVALL\H-AEP045	0.05	-11	27	143
0050	Imperial Valley-06	Agrarias	1979	6.53	1.17	-0.05	IQD	-	IMPVALL\H-AGR003	0.05	-11	28	143
0050	Imperial Valley-06	Bonds Corner	1979	6.53	1.02	0.16	AQD	D	IMPVALL\H-BCR140	0.1	40	29	143
0050	Imperial Valley-06	Brawley Airport	1979	6.53	10.13	0.95	AQD	D	IMPVALL\H-BRA225	0.1	40	30	143
0050	Imperial Valley-06	Calexico Fire Station	1979	6.53	12.16	0.33	AQD	D	IMPVALL\H-CXO225	0.2	40	31	143
0050	Imperial Valley-06	EC Meloland Overpass FF	1979	6.53	1.78	0.51	IDD	D	IMPVALL\H-EMO000	0.1	40	32	143
0050	Imperial Valley-06	El Centro Array #10	1979	6.53	7.88	0.66	AQD	D	IMPVALL\H-E10050	0.1	40	33	143
0050	Imperial Valley-06	El Centro Array #11	1979	6.53	14.16	0.68	AQD	D	IMPVALL\H-E11140	0.2	40	34	143
0050	Imperial Valley-06	El Centro Array #4	1979	6.53	5.45	0.7	IQD	D	IMPVALL\H-E04140	0.1	40	35	143
0050	Imperial Valley-06	El Centro Array #5	1979	6.53	2.31	0.73	IQD	D	IMPVALL\H-E05140	0.1	40	36	143
0050	Imperial Valley-06	El Centro Array #6	1979	6.53	0.33	0.72	IQD	D	IMPVALL\H-E06140	0.1	40	37	143
0050	Imperial Valley-06	El Centro Array #7	1979	6.53	2.27	0.72	AQD	D	IMPVALL\H-E07140	0.1	40	38	143
0050	Imperial Valley-06	El Centro Array #8	1979	6.53	5.57	0.72	AQD	D	IMPVALL\H-E08140	0.1	40	39	143
0050	Imperial Valley-06	El Centro Differential Array	1979	6.53	6.8	0.69	IQD	D	IMPVALL\H-EDA270	0.1	40	40	143
0050	Imperial Valley-06	El Centro Imp. Co. Cent	1979	6.53	9.02	0.73	AQD	D	IMPVALL\H-ECC002	0.1	35	41	143
0050	Imperial Valley-06	Holtville Post Office	1979	6.53	6.06	0.5	AQD	D	IMPVALL\H-HVP225	0.1	40	42	143
0050	Imperial Valley-06	Parachute Test Site	1979	6.53	15.32	0.95	AQD	C	IMPVALL\H-PTS225	0.1	40	43	143
0050	Imperial Valley-06	SAHOP Casa Flores	1979	6.53	11.35	0.13	I-C	D	IMPVALL\H-SHP000	0.2	-11	44	143
0116	Superstition Hills-02	Parachute Test Site	1987	6.54	0.95	-0.8	AQD	C	SUPERST\B-PTS225	0.12	20	45	127

0116	Superstition Hills-02	Westmorland Fire Sta	1987	6.54	13.03	-0.73	ADD	D	SUPERST\B-WSM090	0.1	35	46	127
0127	Northridge-01	Canoga Park - Topanga Can	1994	6.69	14.7	-0.25	--D	D	NORTHR\CNP106	0.05	30	47	122
0127	Northridge-01	Canyon Country - W Lost Cany	1994	6.69	12.44	-0.15	--D	D	NORTHR\LOS000	0.1	30	48	122
0127	Northridge-01	Jensen Filter Plant	1994	6.69	5.43	-0.1	--D	C	NORTHR\JEN022	0.2	-11	49	122
0127	Northridge-01	Newhall - Fire Sta	1994	6.69	5.92	-0.5	AQD	D	NORTHR\NWH090	0.12	23	50	122
0127	Northridge-01	Northridge - 17645 Saticoy St	1994	6.69	12.09	0.15	--D	D	NORTHR\STC090	0.1	30	51	122
0127	Northridge-01	Rinaldi Receiving Sta	1994	6.69	6.53	0.08	--C	D	NORTHR\RRS228	11	-11	52	122
0127	Northridge-01	Sepulveda VA	1994	6.69	8.44	0.19	--D	D	NORTHR\SPV270	0.1	-11	53	122
0127	Northridge-01	Sylmar - Converter Sta	1994	6.69	5.35	-0.07	--D	D	NORTHR\SCS052	11	-11	54	122
0127	Northridge-01	Sylmar - Converter Sta East	1994	6.69	5.19	-0.03	--D	D	NORTHR\SCE018	11	-11	55	122
0127	Northridge-01	Sylmar - Olive View Med FF	1994	6.69	5.3	0.08	AQD	C	NORTHR\SYL090	0.12	23	56	122
0129	Kobe, Japan	KJMA	1995	6.9	0.84	-0.28	--B	C	KOBE\KJM000	0.05	-11	57	230
0118	Loma Prieta	Capitola	1989	6.93	15.23	-0.01	AQC	D	LOMAP\CAP000	0.2	40	58	128
0118	Loma Prieta	Corralitos	1989	6.93	3.85	0.12	APB	C	LOMAP\CLS000	0.2	40	59	128
0118	Loma Prieta	Gilroy - Historic Bldg.	1989	6.93	10.97	0.5	BQD	-	LOMAP\GOF090	0.2	38	60	128
0118	Loma Prieta	Saratoga - W Valley Coll.	1989	6.93	9.31	-0.5	AQD	C	LOMAP\WVC000	0.1	38	61	128
0123	Cape Mendocino	Petrolia	1992	7.01	9.59	0.03	IMD	D	CAPEMEND\PET000	0.07	23	62	340
0138	Duzce, Turkey	Duzce	1999	7.14	11.42	0.08	A-D	D	DUZCE\DZC180	0.08	50	63	265
0125	Landers	Joshua Tree	1992	7.28	10.13	-0.11	AGC	C	LANDERS\JOS000	0.07	23	64	355
0125	Landers	Morongo Valley	1992	7.28	15.26	-0.16	AHC	C	LANDERS\MVH000	11	-11	65	355
0046	Tabas, Iran	Dayhook	1978	7.35	13.94	-0.01	ABB	-	TABAS\DAY280	0.1	-11	66	330
0046	Tabas, Iran	Tabas	1978	7.35	1.2	0.62	ABC	-	TABAS\TAB074	0.05	-11	67	330
0136	Kocaeli, Turkey	Arcelik	1999	7.51	11.67	0.28	B-B	C	KOCAELI\ARC000	0.07	50	68	274
0136	Kocaeli, Turkey	Duzce	1999	7.51	9.35	-0.5	A-D	D	KOCAELI\DZC180	11	15	69	274
0136	Kocaeli, Turkey	Yarimca	1999	7.51	2.96	0.11	B-D	D	KOCAELI\YPT060	0.07	50	70	274

Table 1. "Near-source" earthquake ground motion records selected from PEER database.

EQID	EQNAME	STANAME	YEAR	Mw	Clst Dis	X	GM Site Code	NEHRP	Filename	Max fcHP	Min fcLP	#	Strike
0048	Coyote Lake	San Juan Bautista, 24 Polk St	1979	5.74	19.32	-1	AQD	C	COYOTELK\SJB213	0.2	20	1	336
0102	Chalfant Valley-01	Bishop - LADWP South St	1986	5.77	23.43	0	AQD	-	CHALFANT\B-LAD180	0.11	20	2	48
0102	Chalfant Valley-01	Lake Crowley - Shehorn Res.	1986	5.77	26.9	0	AAB	-	CHALFANT\B-SHE009	0.16	25	3	48
0101	N. Palm Springs	San Jacinto Vall. Cem	1986	6.06	30.97	0.53	AQD	D	PALMSPR\H06270	0.2	31	4	287
0090	Morgan Hill	Agnews State Hospital	1984	6.19	24.49	0.02	AQD	D	MORGAN\AGW240	0.2	13	5	148
0090	Morgan Hill	Corralitos	1984	6.19	23.24	-0.71	APB	C	MORGAN\CLS220	0.2	24	6	148
0090	Morgan Hill	Hollister Diff Array #1	1984	6.19	26.43	-0.98	IQD	D	MORGAN\HD1165	0.2	30	7	148
0090	Morgan Hill	Hollister Diff Array #3	1984	6.19	26.43	-0.98	IQD	D	MORGAN\HD3165	0.2	30	8	148
0090	Morgan Hill	Hollister Diff Array #4	1984	6.19	26.43	-0.98	IQD	D	MORGAN\HD4165	0.2	30	9	148
0090	Morgan Hill	Hollister Diff Array #5	1984	6.19	26.43	-0.98	IQD	D	MORGAN\HD5165	0.2	30	10	148
0090	Morgan Hill	Hollister Diff. Array	1984	6.19	26.43	-0.98	IQD	D	MORGAN\HDA165	0.2	23	11	148
0090	Morgan Hill	San Juan Bautista, 24 Polk St	1984	6.19	27.15	-0.98	AQD	C	MORGAN\SJB213	0.1	21	12	148
0103	Chalfant Valley-02	McGee Creek - Surface	1986	6.19	29.2	-0.63	IQC	-	CHALFANT\A-MCG270	0.1	35	13	148
0064	Victoria, Mexico	SAHOP Casa Flores	1980	6.33	31.25	0.95	I-C	D	VICT\SHP010	0.2	27	14	130
0064	Victoria, Mexico	Victoria Hospital Sotano	1980	6.33	35.2	0.95	--D	-	VICT\HPB000	0.2	26	15	130
0076	Coalinga-01	Parkfield - Fault Zone 12	1983	6.36	30.53	0.6	IHC	-	COALINGA\H-PRK090	0.2	20	16	145
0076	Coalinga-01	Parkfield - Fault Zone 14	1983	6.36	30.79	0.6	IHC	-	COALINGA\H-Z14000	0.2	23	17	145
0076	Coalinga-01	Parkfield - Fault Zone 15	1983	6.36	30.82	0.6	IQB	-	COALINGA\H-Z15000	0.2	20	18	145
0076	Coalinga-01	Parkfield - Fault Zone 16	1983	6.36	29.08	0.6	IQC	-	COALINGA\H-Z16000	0.2	26	19	145
0076	Coalinga-01	Parkfield - Fault Zone 9	1983	6.36	32.84	0.6	IPB	-	COALINGA\H-Z09000	0.2	23	20	145
0076	Coalinga-01	Parkfield - Vineyard Cany 1E	1983	6.36	28.01	0.6	IQC	-	COALINGA\H-PV1000	0.2	23	21	145
0076	Coalinga-01	Parkfield - Vineyard Cany 2W	1983	6.36	31.87	0.6	IHC	-	COALINGA\H-VC2000	0.2	30	22	145
0076	Coalinga-01	Parkfield - Vineyard Cany 4W	1983	6.36	35.94	0.6	IMB	-	COALINGA\H-VC4000	0.2	27	23	145
0050	Imperial Valley-06	Calipatria Fire Station	1979	6.53	25	0.95	BQD	D	IMPVALL\H-CAL225	0.1	40	24	143
0050	Imperial Valley-06	Cerro Prieto	1979	6.53	23.3	-0.05	AVA	C	IMPVALL\H-CPE147	0.1	-11	25	143
0050	Imperial Valley-06	Chihuahua	1979	6.53	17.08	-0.05	IQD	D	IMPVALL\H-CHI012	0.05	-11	26	143
0050	Imperial Valley-06	Compuertas	1979	6.53	20.9	-0.05	IQD	D	IMPVALL\H-CMP015	0.2	-11	27	143
0050	Imperial Valley-06	Delta	1979	6.53	31.94	-0.05	IQD	D	IMPVALL\H-DLT262	0.05	-11	28	143
0050	Imperial Valley-06	El Centro Array #1	1979	6.53	20.31	0.76	AQD	D	IMPVALL\H-E01140	0.1	40	29	143
0050	Imperial Valley-06	El Centro Array #12	1979	6.53	19.65	0.66	IQD	D	IMPVALL\H-E12140	0.1	40	30	143
0050	Imperial Valley-06	El Centro Array #13	1979	6.53	23.69	0.71	AQD	D	IMPVALL\H-E13140	0.2	40	31	143
0050	Imperial Valley-06	Plaster City	1979	6.53	32.44	0.95	AQD	D	IMPVALL\H-PLS045	0.1	40	32	143
0050	Imperial Valley-06	Superstition Mtn Camera	1979	6.53	27.25	0.95	AGB	C	IMPVALL\H-SUP045	0.1	40	33	143
0050	Imperial Valley-06	Westmorland Fire Sta	1979	6.53	16.82	0.95	ADD	D	IMPVALL\H-WSM090	0.1	40	34	143
0116	Superstition Hills-02	Brawley Airport	1987	6.54	17.03	-0.9	AQD	D	SUPERST\B-BRA225	0.13	20	35	127
0116	Superstition Hills-02	El Centro Imp. Co. Cent	1987	6.54	18.2	-0.9	AQD	D	SUPERST\B-ICC000	0.1	38	36	127
0116	Superstition Hills-02	Wildlife Liquef. Array	1987	6.54	23.85	-0.86	IQD	-	SUPERST\B-IVW090	0.1	40	37	127
0030	San Fernando	LA - Hollywood Stor FF	1971	6.61	22.77	-0.64	IPD	D	SFERN\PEL090	0.2	35	38	290
0127	Northridge-01	Lake Hughes #1	1994	6.69	35.81	-0.78	APC	C	NORTHR\L01000	0.12	23	39	122
0127	Northridge-01	Lake Hughes #12A	1994	6.69	21.36	-0.78	IHC	C	NORTHR\H12090	0.12	46	40	122
0127	Northridge-01	Lake Hughes #4 - Camp Mend	1994	6.69	31.66	-0.78	IGB	C	NORTHR\L04000	0.12	23	41	122
0127	Northridge-01	Lake Hughes #4B - Camp Mend	1994	6.69	31.69	-0.78	IGB	C	NORTHR\L4B000	0.12	23	42	122
0127	Northridge-01	Lake Hughes #9	1994	6.69	25.36	-0.78	AGA	C	NORTHR\L09000	0.08	-11	43	122
0127	Northridge-01	Pacific Palisades - Sunset	1994	6.69	24.08	0.22	--B	C	NORTHR\SUN190	0.05	30	44	122
0127	Northridge-01	Santa Susana Ground	1994	6.69	16.74	-0.76	--A	C	NORTHR\SSU000	11	-11	45	122

0127	Northridge-01	Stone Canyon	1994	6.69	29.21	-0.78	---	C	NORTHR\SCR000	0.03	-11	46	122
0127	Northridge-01	Vasquez Rocks Park	1994	6.69	23.64	0.04	IBA	C	NORTHR\VAS000	0.08	-11	47	122
0129	Kobe, Japan	Abeno	1995	6.9	24.75	-0.61	--D	D	KOBE\ABN000	0.05	40	48	230
0129	Kobe, Japan	Tadoka	1995	6.9	31.59	-0.31	--D	D	KOBE\TDO000	0.05	40	49	230
0129	Kobe, Japan	Yae	1995	6.9	27.68	-0.63	--D	-	KOBE\YAE000	0.05	-11	50	230
0118	Loma Prieta	Agnews State Hospital	1989	6.93	24.57	-0.5	AQD	D	LOMAP\AGW000	0.2	30	51	128
0118	Loma Prieta	Anderson Dam (Downstream)	1989	6.93	20.26	0.23	AFD	C	LOMAP\AND270	0.2	40	52	128
0118	Loma Prieta	Anderson Dam (L Abut)	1989	6.93	20.26	0.23	AQA	C	LOMAP\ADL250	0.1	32	53	128
0118	Loma Prieta	Coyote Lake Dam (Downst)	1989	6.93	20.8	0.44	IHD	C	LOMAP\CLD195	0.1	29	54	128
0118	Loma Prieta	Gilroy Array #6	1989	6.93	18.33	0.5	IKB	C	LOMAP\GO6000	0.2	31	55	128
0118	Loma Prieta	Halls Valley	1989	6.93	30.49	-0.22	IFC	D	LOMAP\HVR000	0.2	22	56	128
0118	Loma Prieta	UCSC	1989	6.93	18.51	-0.25	--B	-	LOMAP\UC2000	0.1	-11	57	128
0118	Loma Prieta	UCSC Lick Observatory	1989	6.93	18.41	-0.24	AKA	C	LOMAP\LOB000	0.2	40	58	128
0118	Loma Prieta	WAHO	1989	6.93	17.47	-0.08	AQD	-	LOMAP\WAH000	0.1	-11	59	128
0123	Cape Mendocino	Fortuna - Fortuna Blvd	1992	7.01	18.45	0.78	IQD	C	CAPEMEND\FOR000	0.07	23	60	340
0123	Cape Mendocino	Rio Dell Overpass - FF	1992	7.01	17.76	0.63	APC	C	CAPEMEND\RIO270	0.07	23	61	340
0125	Landers	Barstow	1992	7.28	34.85	0.76	IQD	C	LANDERS\BRS000	0.07	23	62	355
0125	Landers	Desert Hot Springs	1992	7.28	16.44	-0.16	AQD	C	LANDERS\DSP000	0.07	23	63	355
0125	Landers	Mission Creek Fault	1992	7.28	20.59	-0.16	---	C	LANDERS\MCF000	11	-11	64	355
0125	Landers	North Palm Springs	1992	7.28	21.68	-0.16	AHD	C	LANDERS\NPS000	11	-11	65	355
0125	Landers	Palm Springs Airport	1992	7.28	30.26	-0.16	IQD	D	LANDERS\PSA000	0.07	23	66	355
0125	Landers	Yermo Fire Station	1992	7.28	23.28	0.76	AQD	D	LANDERS\YER270	0.07	23	67	355
0046	Tabas, Iran	Boshrooyeh	1978	7.35	28.79	0.66	--C	-	TABAS\BOS079	0.04	20	68	330
0136	Kocaeli, Turkey	Goynuk	1999	7.51	33.7	-0.33	--B	-	KOCAELI\GYN000	0.15	25	69	274
0136	Kocaeli, Turkey	Iznic	1999	7.51	33.12	0.1	A-D	D	KOCAELI\IZN180	0.1	25	70	274

Table 2. "Ordinary" earthquake ground motion records selected from PEER database.

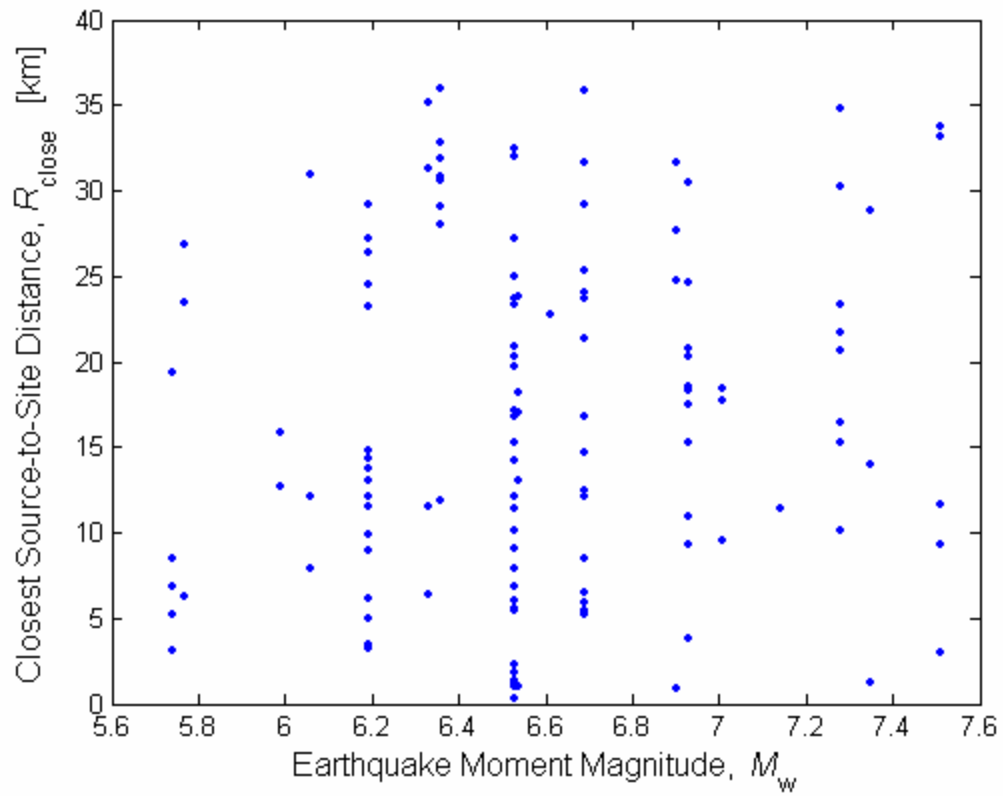


Figure 1. Magnitudes and distances for the 140 earthquake ground motion records considered.

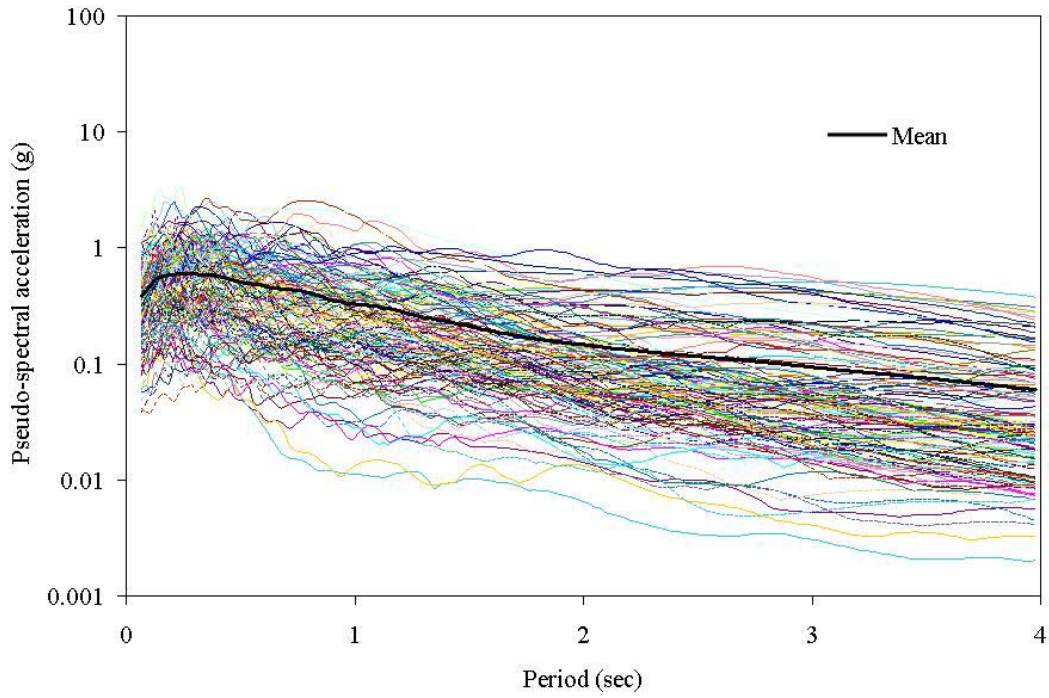


Figure 2. Pseudo-spectral acceleration versus period for the 140 earthquake ground motion records considered.

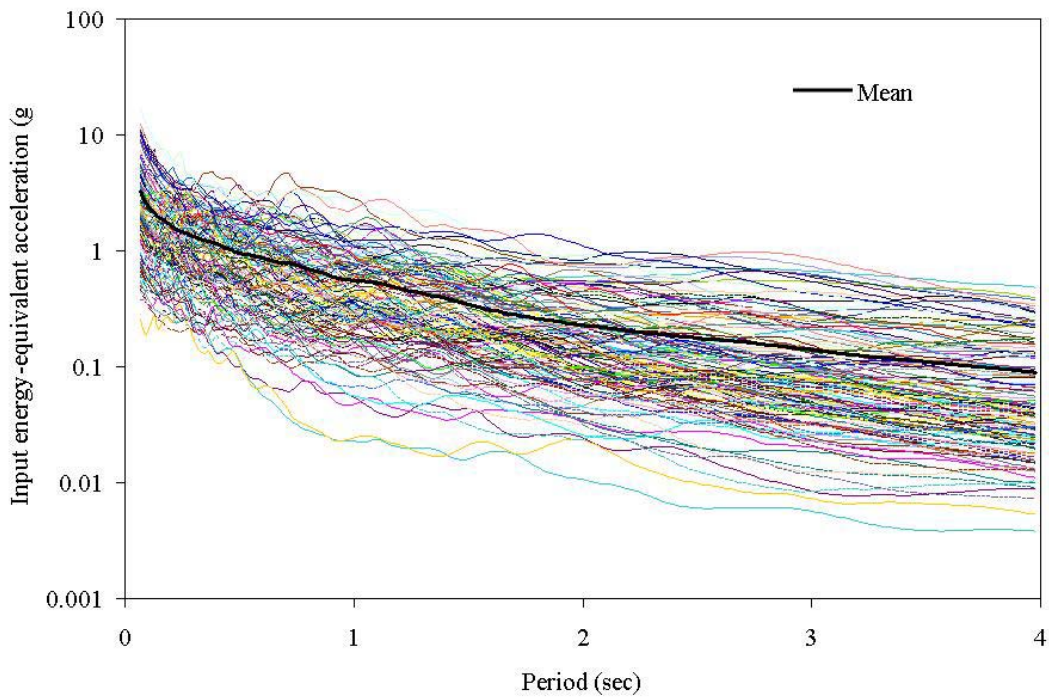


Figure 3. Input energy-equivalent acceleration versus period for the 140 earthquake ground motion records considered.

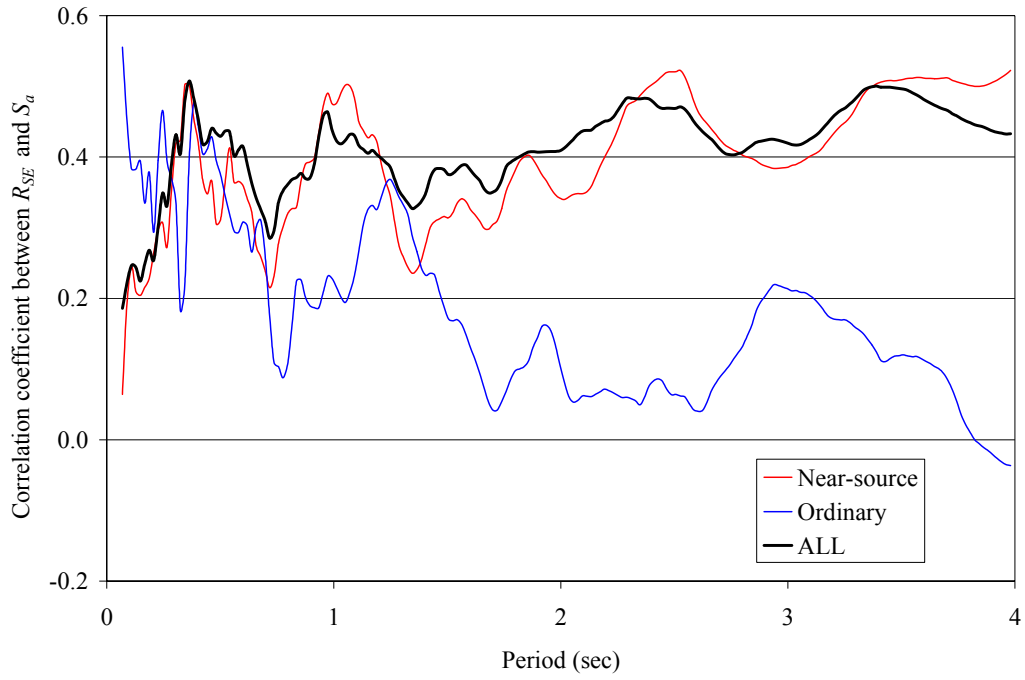


Figure 4. Correlation coefficient between $R_{SE}(f)$ and $S_a(f)$ for the ground motion records considered.

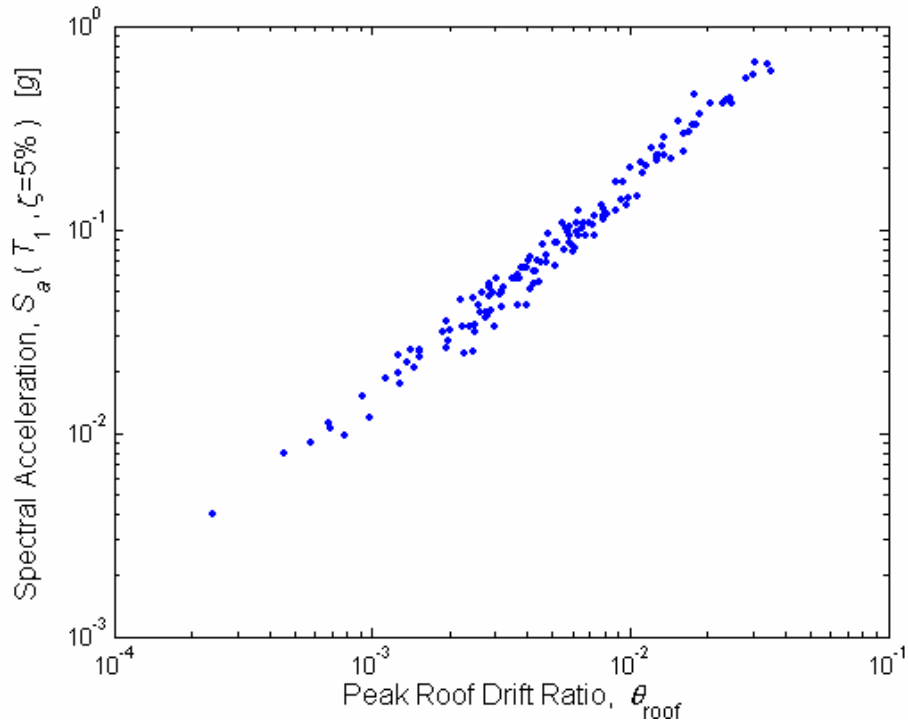


Figure 5. Roof drift response of the ductile 9-story building model to the 140 selected earthquake records (computed via nonlinear dynamic analysis).

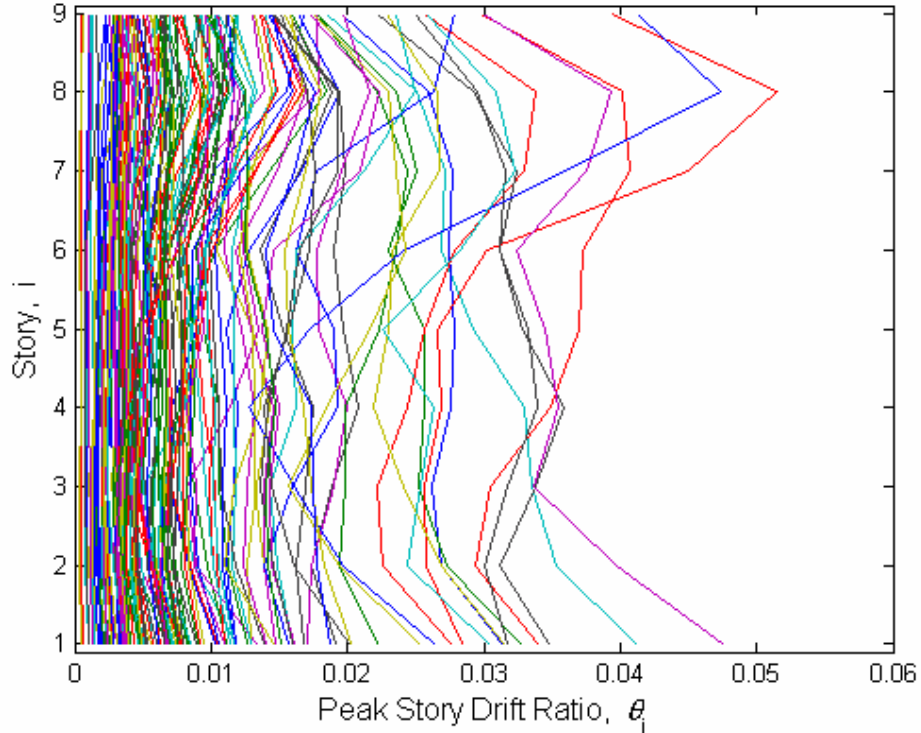


Figure 6. Story drift response of the ductile 9-story building model to the 140 selected earthquake records (computed via nonlinear dynamic analysis).

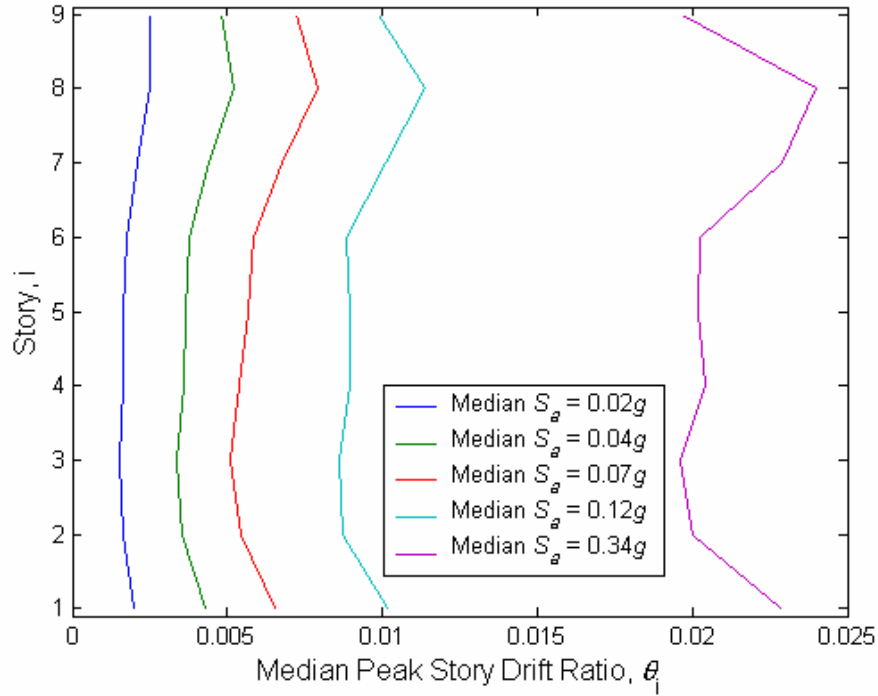


Figure 7. Median story drift response of the ductile 9-story building model for 5 bins of 28 earthquake records sorted according to first-mode spectral acceleration.

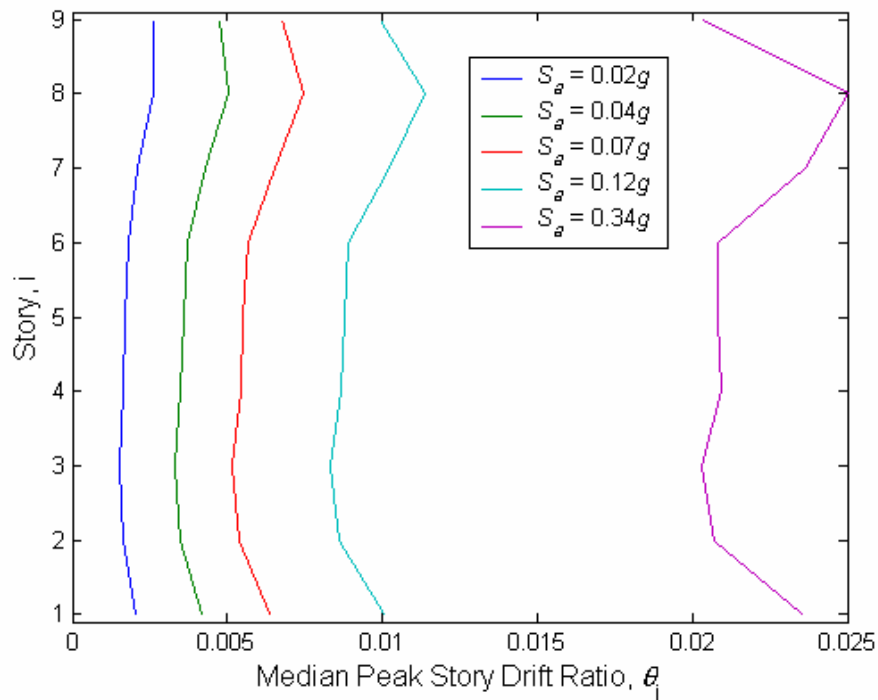


Figure 8. Median story drift response of the ductile 9-story building model, as predicted by the regression of θ_i on $S_a(f_i)$, for the same five first-mode spectral acceleration values shown in Figure 7.